PERGAMON

International Journal of Heat and Mass Transfer 43 (2000) 1699–1713

International Journal of HEAT and MASS TRANSFER

www.elsevier.com/locate/ijhmt

# An extension of the weighted sum of gray gases non-gray gas radiation model to a two phase mixture of non-gray gas with particles

Myoung Jong Yu, Seung Wook Baek*, Jae Hyun Park

*Department of Aerospace Engineering, Korea Advanced Institute of Science and Technology, 373-1 Kusung-dong, Yusung-Gu, Taejon 305-701, South Korea*

Received 6 May 1999; received in revised form 16 August 1999

## Abstract

A great deal of efforts has been exercised to date to accurately model the non-gray behavior of the gases. Among others, the weighted sum of gray gases model (WSGGM), which replaces the non-gray gas behavior by an equivalent finite number of gray gases, is a simplified model yielding reasonable results. However, a discussion on the weighting factors required for an estimation of radiation in a mixture of non-gray gas/gray particulate is not yet established for WSGGM, since they are dependent on the particle number density, particle size distribution, local temperature and partial pressure. Consequently, the relation between the weighting factors used in the WSGGM for a mixture of non-gray gas and gray particles with scattering in the thermal non-equilibrium has been discussed here, which has not been done before to the author's best knowledge. Weighting factors for the particles, of which temperature is different from that of the gas, were evaluated analytically for the WSGGM. The results were, then, validated for the problem of isothermal gas containing soot particulates between two parallel slab walls. For further application, the approach derived here was implemented to examine the non-gray radiative effects of the two phase mixture in an axisymmetric cylinder by changing such various parameters as the particle temperature, non-gray gas composition and particle concentration. The effects of thermal non-equilibrium in a mixture of gas and particles were also discussed in parallel with scattering effects by particles. Parametric study showed that a variation in the gas concentration yielded a noticeable change in the radiative heat transfer when the suspended particle temperature was different from the gas temperature. New contribution of this study consisted in an extension of applicability of the WSGGM non-gray model to two phase radiation. 

*Keywords:* Non-gray; Radiation; Two phase; WSGGM; Weighting factors

## 1. Introduction

Two phase mixture is very common in engineering practice, for example, particle-gas heat exchanger, pulverized coal furnace, solid rocket motor etc. Since various radiating gases, soot particles and poly-dispersed particulates are involved in diverse thermal processes, the thermal radiation is considered to play as significant a role as the other heat transfer mode does. Nevertheless, its complete modelling is far from being complete due to various complexities in dealing with

* Corresponding author. Tel.: +82-42-869-3714; fax: +82-42-869-3710.

*E-mail address:* swbaek@sorak.kaist.ac.kr (S.W. Baek).

0017-9310/00/$ - see front matter 
PII: S0017-9310(99)00265-3

**Nomenclature**

| | |
|---|---|
| $d$ | particle diameter [m] |
| $E_b$ | blackbody emissive power [W/m$^2$] |
| $I$ | radiation intensity [W/(m$^2$ sr)] |
| $q$ | heat flux [W/m$^2$] |
| $\hat{s}$ | angular direction |
| $s$ | distance travelled |
| $T$ | temperature [K] |
| $w$ | weighting factor in WSGGM |

*Greek symbols*

| | |
|---|---|
| $\varepsilon$ | emissivity |
| $\kappa$ | absorption coefficient [m$^{-1}$] |
| $\sigma_{sp}$ | scattering coefficient [m$^{-1}$] |
| $\sigma$ | Stefan–Boltzmann constant [$5.67 \times 10^{-8}$ W/(m$^2$ K$^4$)] |
| $\Phi$ | scattering phase function |

*Superscript*

| | |
|---|---|
| $'$ | incident direction |

*Subscripts*

| | |
|---|---|
| b | blackbody |
| g | gas |
| p | particle |
| s | soot |
| w | wall |
| $\eta$ | wave number |

radiative properties of non-gray gases, multi-dimensional complex geometry, and computational efficiency as well as accuracy.

Due to its rudimental difficulties in handling the spectral dependency of the radiation, its modelling usually adopts a simple gray gas assumption as done in many problems related to thermal radiation [1–4]. However, the non-gray gases like water vapor and carbon dioxide are necessarily produced in the industrial energy systems so that a great deal of efforts has been exercised to date to accurately model the non-gray behavior of the gases. Among others, the weighted sum of gray gases model (WSGGM), which replaces the non-gray gas behavior by an equivalent finite number of gray gases, is one of the simplified models reasonably used in a practical application. Since Hottel and Sarofim [5] developed its concept in the context of the zonal method, it has been applied to examine the effects of the radiation in a spray combustion system [6] and gas-fired furnaces [7]. Smith et al. [8] and Coppalle and Vervish [9] and others investigated a determination of the weighting factors required for WSGGM. An error induced in the total emissivity was found to be within 5–10% compared with the line-by-line spectral analysis [10]. However, the evaluation of the weighting factors required for an estimation of radiation in a mixture of non-gray gas/gray particulate is not yet established, since they are dependent on the particle number density, particle size distribution, local temperature and partial pressure. Denison and Webb [11] used a hybrid model of $k$-distribution and weighted sum of gray gases to estimate a spectrally integrated radiative transfer rate in non-gray gas with particles, while neglecting the temperature difference between gas and particles. It is still not clear whether the WSGGM can be directly applicable to solving the problems with particles-suspended mixture when a thermal equilibrium between gas and particles is not assumed.

A lot of previous works that dealt with thermal problems between gas and particles have been reported for scientific equipment [12] as well as industrial energy systems [4,13–16]. However, most of the radiation submodels therein considered that the particle and gas temperatures are the same so that a thermal equilibrium between them is assumed. Modest [17], though, suggested that the gray gas assumption be acceptable if the particle size distribution in suspension is diverse. The effect of separate char/coal particle and gas temperature on the radiative heat flux incident to the boiler wall of industrial scale has been examined by Denison and Webb [18]. Using the geometric mean beam length approach for the radiative properties, it was found that the particle temperature, which is different from the local gas temperature, has a significant effect on the radiative heat flux on the furnace walls.

But for the industrial heat processing or generating systems with complex geometry, it is not still clear how to specify the geometric mean beam length. Yuen and Ma [19] showed that even for the one-dimensional geometry, the geometric mean beam length approach can lead to a significant error especially when the scattering is present. Consequently, a more significant error could be induced for multi-dimensional industrial heat generating systems, for which the specification of the appropriate geometric mean beam length would be more difficult. A difficulty in defining the effective geometric mean beam length can be circumvented by using the WSGGM for practical applications, based on the local partial pressure and temperature within a given range of partial pressure-path length products. For the case of two phase mixture in thermal non-equilibrium, an appropriate specification of the weighting factors still remains to be resolved. Once done, the concepts of WSGGM used for the single phase gas radiation can be applied to attack the non-gray radiation for the two phase mixture problems in thermal non-equilibrium.

The main objective in this study is to theoretically derive the relation between the weighting factors used in the WSGGM for a mixture of non-gray gas and gray particles with scattering in the thermal non-equilibrium, which has not been discussed before to the author's best knowledge. The results are, then, validated for the problem of isothermal gas containing soot particulates between two parallel slab walls. For further application, the approach derived here is implemented to examine the non-gray radiative effects of the two phase mixture in an axisymmetric cylinder by changing such various parameters as the particle temperature, non-gray gas composition and particle concentration.

## 2. Mathematical formulations

When some emitting and scattering particles as well as non-scattering soot particulates are suspended in the radiative gas medium, the radiative transfer equation (RTE) governing the spectral change of radiative intensity can be written by

$$\frac{\mathrm{d}I_\eta}{\mathrm{d}s} = -(\kappa_{\mathrm{g},\eta} + \kappa_{\mathrm{p},\eta} + \kappa_{\mathrm{s},\eta} + \sigma_{\mathrm{sp},\eta})I_\eta + \kappa_{\mathrm{g},\eta} I_{\mathrm{b},g\eta} + \kappa_{\mathrm{p},\eta} I_{\mathrm{b},p\eta} + \kappa_{\mathrm{s},\eta} I_{\mathrm{b},s\eta} + \frac{\sigma_{\mathrm{sp},\eta}}{4\pi}\int_{4\pi} \Phi_\eta(\hat{s},\hat{s}')I_\eta(\hat{s}')\,\mathrm{d}\Omega' \tag{1}$$

where $\kappa_{\mathrm{g},\eta}$, $\kappa_{\mathrm{p},\eta}$ and $\kappa_{\mathrm{s},\eta}$ are the absorption coefficients of gas, particles and soot at the specific wave number $\eta$ respectively. Integrating of Eq. (1) over the $j$th wave number range for an arbitrary $k$th gray band as shown in Fig. 1 gives

$$\begin{aligned}\int_{\eta_{j-}^k}^{\eta_{j+}^k}\left(\frac{\mathrm{d}I_\eta}{\mathrm{d}s}\right)\mathrm{d}\eta &= \int_{\eta_{j-}^k}^{\eta_{j+}^k}\left[-(\kappa_{\mathrm{g},\eta} + \kappa_{\mathrm{p},\eta} + \kappa_{\mathrm{s},\eta} + \sigma_{\mathrm{sp},\eta})I_\eta + \kappa_{\mathrm{g},\eta} I_{\mathrm{b,g}\eta} + \kappa_{\mathrm{p},\eta} I_{\mathrm{b,p}\eta} + \kappa_{\mathrm{s},\eta} I_{\mathrm{b,s}\eta}\right]\mathrm{d}\eta \\ &\quad + \int_{\eta_{j-}^k}^{\eta_{j+}^k}\left[\frac{\sigma_{\mathrm{sp},\eta}}{4\pi}\int_{4\pi}\Phi_\eta(\hat{s},\hat{s}')I_\eta(\hat{s}')\,\mathrm{d}\Omega'\right]\mathrm{d}\eta\end{aligned} \tag{2}$$

By applying Lorentz's rule, the left-hand side of Eq. (2) becomes

$$\int_{\eta_{j-}^k}^{\eta_{j+}^k}\left(\frac{\mathrm{d}I_\eta}{\mathrm{d}s}\right)\mathrm{d}\eta = \frac{\mathrm{d}}{\mathrm{d}s}\int_{\eta_{j-}^k}^{\eta_{j+}^k} I_\eta \mathrm{d}\eta - \left[\frac{\mathrm{d}\eta_{j+}^k}{\mathrm{d}s} I_\eta\left(\eta_{j+}^k\right) - \frac{\mathrm{d}\eta_{j-}^k}{\mathrm{d}s} I_\eta\left(\eta_{j-}^k\right)\right]. \tag{3}$$

If the wave number boundaries are fixed, the last two terms on the right-hand side of Eq. (3) will disappear [20]. After a substitution of Eq. (3) into the left-hand side of the Eq. (2) and rearrangement, the radiative transfer equation for the $k$th gray band can be written as follows

$$\frac{\mathrm{d}I_k}{\mathrm{d}s} = -(\kappa_{\mathrm{g},k} + \kappa_{\mathrm{p},k} + \kappa_{\mathrm{s},k} + \sigma_{\mathrm{sp},k})I_k + \kappa_{\mathrm{g},k} w_{\mathrm{g},k} I_{\mathrm{b,g}} + \kappa_{\mathrm{p},k} w_{\mathrm{p},k} I_{\mathrm{b,p}} + \kappa_{\mathrm{s},k} w_{\mathrm{s},k} I_{\mathrm{b,s}} + \frac{\sigma_{\mathrm{sp},k}}{4\pi}\int_{4\pi}\Phi(\hat{s},\hat{s}')I_k(\hat{s}')\,\mathrm{d}\Omega' \tag{4}$$

where $\kappa_{\mathrm{g},k}$, $\kappa_{\mathrm{p},k}$ and $\kappa_{\mathrm{s},k}$ are the spatially dependent absorption coefficients of gas, particles and soot for the $k$th gray band. Corresponding weighting factors for gas, particles, and soot as a function of temperature and position also are represented by

$$w_{\mathrm{g},k} = \frac{\sum_j \int_{\eta_{j-}^k}^{\eta_{j+}^k} E_{\mathrm{g,b}\eta}(T_\mathrm{g},\eta)\,\mathrm{d}\eta}{E_{\mathrm{g,b}}(T_\mathrm{g})}, \tag{5}$$

$$w_{\mathrm{p},k} = \frac{\sum_j \int_{\eta_{j-}^k}^{\eta_{j+}^k} E_{\mathrm{p,b}\eta}(T_\mathrm{p},\eta)\,\mathrm{d}\eta}{E_{\mathrm{p,b}}(T_\mathrm{p})}, \tag{6}$$

and

$$w_{\mathrm{s},k} = \frac{\sum_j \int_{\eta_{j-}^k}^{\eta_{j+}^k} E_{\mathrm{s,b}\eta}(T_\mathrm{s},\eta)\,\mathrm{d}\eta}{E_{\mathrm{s,b}}(T_\mathrm{s})} \tag{7}$$

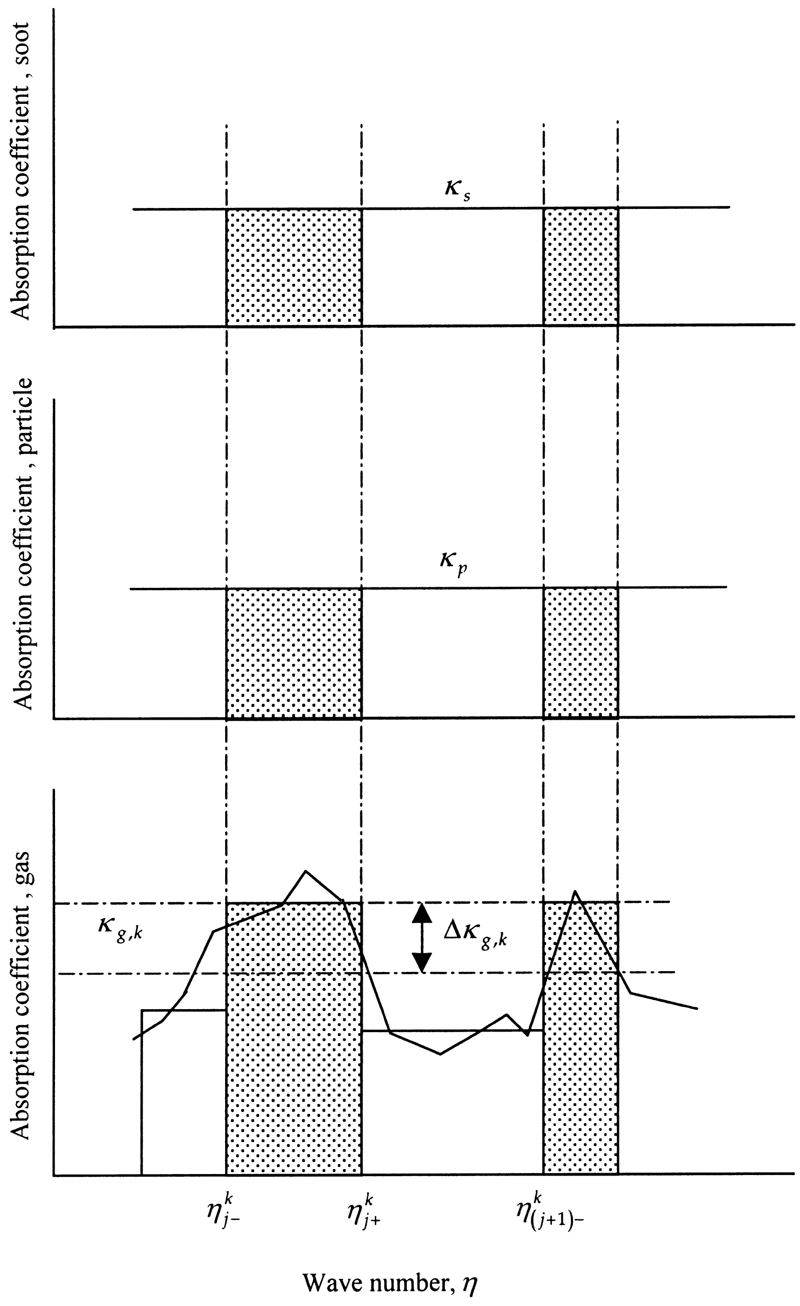


Fig. 1. Weighted sum of gray gas model spectrum in a mixture of non-gray gas, gray soot, and other gray particles.

where the Plank's function is defined by

$$E_{b\eta} \equiv \frac{2\pi h c_o^2 \eta^3}{e^{hc_o\eta/k_B T} - 1} \tag{8}$$

Eq. (4) would be reasonable when each gas band is narrow as well as non-overlapping and furthermore, the absorption coefficients for soot, $\kappa_{s,\eta}$ and for particles, $\kappa_{p,\eta}$ do not vary appreciably over each band.

Below, a discussion on the weighting factors is to follow. Different from the approach, which is based on the gas radiation only without scattering as done by Modest [17], this work assumes a mixture of non-gray gases, gray particles, and gray soot particulates so that

$$\kappa_{p,k} = \kappa_p, \kappa_{s,k} = \kappa_s, \sigma_{sp,k} = \sigma_{sp}, \quad k = 1, 2, \ldots, N \tag{9}$$

Even though the particle absorption coefficients depend on such factors as incident electromagnetic wave, incident direction, emission direction etc., Skocypec et al. [21] experimentally showed that the emittance due to particulate can be considered gray so that the postulation above may be acceptable here. By substitution of Eq. (9) into (4), it becomes

$$\frac{\mathrm{d}I_k}{\mathrm{d}s} = -(\kappa_{g,k} + \kappa_p + \kappa_s + \sigma_{sp})I_k + \kappa_{g,k}w_{g,k}I_{b,g} + \kappa_p w_{p,k}I_{b,p} + \kappa_s w_{s,k}I_{b,s} + \frac{\sigma_{sp}}{4\pi}\int_{4\pi}\Phi(\hat{s}',\hat{s})I_k(\hat{s}')\,\mathrm{d}\Omega'. \tag{10}$$

Integration of Eq. (10) over the path length leads to

$$\begin{aligned} I_k(s) = {} & I_{bw}(s_w)\mathrm{e}^{-\int_{s_w}^{s}(\kappa_{g,k}+\kappa_p+\kappa_s+\sigma_{sp})\,\mathrm{d}s''} \\ & + \int_{s_w}^{s} w_{g,k}\kappa_{g,k}I_{b,g}\mathrm{e}^{-\int_{s'}^{s}(\kappa_{g,k}+\kappa_p+\kappa_s+\sigma_{sp})\,\mathrm{d}s''}\,\mathrm{d}s' \\ & + \int_{s_w}^{s} w_{k,p}\kappa_p I_{b,p}\mathrm{e}^{-\int_{s'}^{s}(\kappa_{g,k}+\kappa_p+\kappa_s+\sigma_{sp})\,\mathrm{d}s''}\,\mathrm{d}s' \\ & + \int_{s_w}^{s} w_{k,s}\kappa_s I_{b,s}\mathrm{e}^{-\int_{s'}^{s}(\kappa_{g,k}+\kappa_p+\kappa_s+\sigma_{sp})\,\mathrm{d}s''}\,\mathrm{d}s' \\ & + \int_{s_w}^{s}\left[\frac{\sigma_{sp}}{4\pi}\int_{4\pi}\Phi(\hat{s},\hat{s}')I_k(\hat{s}')\,\mathrm{d}\Omega'\right] \mathrm{e}^{-\int_{s'}^{s}(\kappa_{g,k}+\kappa_p+\kappa_s+\sigma_{sp})\,\mathrm{d}s''}\,\mathrm{d}s'. \end{aligned} \tag{11}$$

Then the total intensity $I(s)$ can be found to sum up all the $k$th gray band intensities such that

$$I(s) = \sum_{k=0}^{N} I_k(s) \tag{12}$$

Based on Eqs. (10) and (11), the WSGGM may be applied to any RTE solver if appropriate values for the absorption and scattering coefficients are retrieved, even though Modest [17] introduced the WSGGM approach without scattering term.

And then, the weighting factors for soot and particles are required to evaluate the $k$th gray intensity, Eq. (11). In order to derive them, the absorption and emission due to soot particulates and the particle scattering are temporarily omitted. Thereby, Eqs. (10) and (12) can be simplified as follows,

$$\frac{\mathrm{d}I_k}{\mathrm{d}s} = -(\kappa_{g,k} + \kappa_p)I_k + \kappa_{g,k}w_{g,k}I_{b,g} + \kappa_p w_{p,k}I_{b,p} \tag{13}$$

$$\begin{aligned} I(s) = {} & \sum_{k=0}^{N} I_k(s) \\ = {} & \sum_{k=0}^{N} I_{bw}(s_w)\mathrm{e}^{-\int_{s_w}^{s}(\kappa_{g,k}+\kappa_p)\,\mathrm{d}s''} \\ & + \sum_{k=0}^{N}\int_{s_w}^{s} w_{g,k}\kappa_{g,k}I_{b,g}\mathrm{e}^{-\int_{s'}^{s}(\kappa_{g,k}+\kappa_p)\,\mathrm{d}s''}\,\mathrm{d}s' \\ & + \sum_{k=0}^{N}\int_{s_w}^{s} w_{p,k}\kappa_p I_{b,p}\mathrm{e}^{-\int_{s'}^{s}(\kappa_{g,k}+\kappa_p)\,\mathrm{d}s''}\,\mathrm{d}s' \end{aligned} \tag{14}$$

Now, for a nonscattering medium with spectral absorption coefficients for gas and particles $\kappa_{g,\eta}$ and $\kappa_{p,\eta}$, the equation of transfer for the radiative intensity $I_\eta$ at a wave number $\eta$ and along a path $s$ becomes

$$\frac{\mathrm{d}I_\eta}{\mathrm{d}s} = -(\kappa_{g,\eta} + \kappa_{p,\eta})I_\eta + \kappa_{g,\eta}I_{g,b\eta} + \kappa_{p,\eta}I_{p,b\eta} \tag{15}$$

Its formal solution is found to be

$$\begin{aligned} I_\eta(s) = {} & I_{\eta w}(s_w)\mathrm{e}^{-\int_{s_w}^{s}(\kappa_{g,\eta}+\kappa_{p,\eta})\,\mathrm{d}s'} \\ & + \int_{s_w}^{s}\kappa_{g,\eta}I_{b,g\eta}\mathrm{e}^{-\int_{s'}^{s}(\kappa_{g,\eta}+\kappa_{p,\eta})\,\mathrm{d}s''}\,\mathrm{d}s' \\ & + \int_{s_w}^{s}\kappa_{p,\eta}I_{b,p\eta}\mathrm{e}^{-\int_{s'}^{s}(\kappa_{g,\eta}+\kappa_{p,\eta})\,\mathrm{d}s''}\,\mathrm{d}s' \end{aligned} \tag{16}$$

where $I_{\eta w}(s_w)$ is the intensity emitted into the medium from the wall. Integration of Eq. (16) over the entire spectrum yields the total intensity as follows

$$\begin{aligned} I(s) = {} & \int_0^\infty I_\eta(s)\,\mathrm{d}\eta \\ = {} & \int_0^\infty I_{\eta w}(s_w)\mathrm{e}^{-\int_{s_w}^{s}(\kappa_{g,\eta}+\kappa_{p,\eta})\,\mathrm{d}s''}\,\mathrm{d}\eta \\ & + \int_{s_w}^{s}\left[\int_0^\infty \kappa_{g,\eta}I_{b,g\eta}\mathrm{e}^{-\int_{s'}^{s}(\kappa_{g,\eta}+\kappa_{p,\eta})\,\mathrm{d}s''}\,\mathrm{d}\eta\right]\mathrm{d}s' \\ & + \int_{s_w}^{s}\left[\int_0^\infty \kappa_{p,\eta}I_{b,p\eta}\mathrm{e}^{-\int_{s'}^{s}(\kappa_{g,\eta}+\kappa_{p,\eta})\,\mathrm{d}s''}\,\mathrm{d}\eta\right]\mathrm{d}s' \end{aligned} \tag{17}$$

If the particles obey gray assumption, the absorption coefficient for particles may be written as

$$\kappa_{p,\eta} = \kappa_p \tag{18}$$

and Eq. (17) becomes

$$I(s) = \left[\int_0^{\infty} I_{\eta w}(s_w) e^{-\int_{s_w}^{s} \kappa_{g,\eta}\, ds''} d\eta\right] \times e^{-\int_{s_w}^{s} \kappa_p\, ds''} + \int_{s_w}^{s}\left[\int_0^{\infty} \kappa_{g,\eta} I_{b,g\eta} e^{-\int_{s'}^{s} \kappa_{g,\eta}\, ds''} d\eta\right] e^{-\int_{s'}^{s} \kappa_p\, ds''} ds' + \int_{s_w}^{s}\left[\int_0^{\infty} \kappa_p I_{p,b\eta} e^{-\int_{s'}^{s} \kappa_{g,\eta}\, ds''} d\eta\right] e^{-\int_{s'}^{s} \kappa_p\, ds''} ds' \tag{19}$$

The spectral emissivity of a participating media is defined by

$$\varepsilon_g(T, s' \to s) = \frac{1}{I_b(T)} \int_0^{\infty}\left[1 - e^{-\int_{s'}^{s} \kappa_{g,\eta}\, ds''}\right] I_{b,g\eta}\, d\eta \tag{20}$$

Substituting Eq. (20) into (19) leads to

$$I(s) = \left[1 - \varepsilon_g(T_w, s_w \to s)\right] I_{bw}(s_w) e^{-\int_{s_w}^{s} \kappa_p\, ds''} - \int_{s_w}^{s} \frac{\partial \varepsilon_g(T_g, s' \to s)}{\partial s'} I_{b,g} e^{-\int_{s'}^{s} \kappa_p\, ds''} ds' + \int_{s_w}^{s}\left[1 - \varepsilon_g(T_p, s' \to s)\right] \times \kappa_p I_{b,p} e^{-\int_{s'}^{s} \kappa_p\, ds''} ds' \tag{21}$$

The absorptivity in Eq. (21) can be approximated by a weighted sum of gray gases such that

$$\varepsilon_g(T, s' \to s) = \sum_{k=1}^{N} w_k(T, \vec{r}, \hat{s})\left[1 - e^{-\kappa_{g,k}(s - s')}\right]. \tag{22}$$

Substituting Eq. (22) into (21) for the case of blackbody wall, Eq. (21) can be represented by

$$I(s) = \sum_{k=0}^{N} I_{bw}(s_w) e^{-\int_{s_w}^{s} (\kappa_{g,k} + \kappa_p)\, ds''} + \sum_{k=0}^{N} \int_{s_w}^{s} w_k(T_g, s' \to s) \kappa_{g,k} I_{b,g} e^{-\int_{s'}^{s} (\kappa_{g,k} + \kappa_p)\, ds''} ds' + \sum_{k=0}^{N} \int_{s_w}^{s} w_k(T_p, s' \to s) \kappa_p I_{b,p} e^{-\int_{s'}^{s} (\kappa_{g,k} + \kappa_p)\, ds''} ds' \tag{23}$$

By comparison of Eq. (14) with (23), it is found that weighting factor for particles has the same functional form as that for gas, corresponding to local temperature and partial pressure. Consequently, if the gas and particles are not in thermal equilibrium, it becomes

$$w_{p,k} = w_{g,k}(T_p). \tag{24}$$

Furthermore, if the gas, particles and soot particulates share all the same $k$th gray bands, even the weighting factors for particles and soot particulates have the same type as that for the gas so that $w_{p,k} = w_{g,k}(T_p)$, $w_{s,k} = w_{g,k}(T_s)$. Then, Eq. (4) can be written by the following simplified form

$$\frac{dI_k}{ds} = -(\kappa_{g,k} + \kappa_p + \kappa_s + \sigma_{sp}) I_k + w_{g,k}(T_g) \kappa_{g,k} I_{b,g} + w_{g,k}(T_s) \kappa_s I_{b,s} + w_{g,k}(T_p) \kappa_p I_{b,p} + \frac{\sigma_{sp}}{4\pi} \int_{4\pi} I_k(s') \Phi(\hat{s}, \hat{s}')\, d\Omega' \tag{25}$$

Modest [17] has shown that the WSGGM can be used with any solution method, replacing the non-gray medium by an equivalent number of gray media with corresponding absorption coefficients. The method of solution of the RTE chosen in this analysis is the discrete ordinates method [22]. The total intensity can be obtained by summing up all of the intensity for each gray band that is obtained by integrating each RTE for the radiative intensity $I_k$ with corresponding weighting factor for each gray band.

## 3. Radiative properties

The WSGGM procedure derived above for mixture can deal with the non-gray effects of the particle scattering as done by Denison and Webb [11], who, though, solved a problem of mixture only in thermal equilibrium using the $k$-distribution method. However, in the further presentation of this study below, only the gray radiation is assumed for the particle absorption and scattering, focusing on the two phase mixture in thermal non-equilibrium as the main objective of this paper. The absorption and scattering coefficients due to particles are defined by [3]

$$\kappa_p = \varepsilon_p \sum_i N_i \frac{\pi d_i^2}{4} \tag{26}$$

$$\sigma_{sp} = (1-\varepsilon_p) \sum_i N_i \frac{\pi d_i^2}{4} \tag{27}$$

The particle emissivity $\varepsilon_p$ is here taken to be an algebraic average of the emissivities of the unburned coal and residual ash as done by Chui et al. [3]. In Eqs. (26) and (27), $N_i$ and $\pi d_i^2/4$ are the particle number density and the particle projected area pertaining to group $i$, respectively.

According to Modest [17], the soot absorption coefficient is defined as

$$\kappa_s = \frac{3.72 f_v C_o T}{C_2}, \mathrm{m}^{-1} \tag{28}$$

where $C_o = 36\pi nk/[(n^2-k^2+2)^2+4n^2k^2]$, $C_2 =$ 1.4388 cm K. While $n = 1.85$ is the real part of the complex index of refraction, $k = 0.22$ is the absorptive index.

## 4. Validation

In this study, the discrete ordinates method (DOM) with the weighted sum of gray gases model (WSGGM) as non-gray model and the scattering phase function is used to solve the radiation for a mixture in thermally non-equilibrium. In order to validate the numerical development derived here, two simplified examples are considered here, since there is no benchmark solution previously solved for a mixture composed of gas, soot and particles.

First of all, a problem of isothermal medium of temperature 1250 K contained between two parallel slab walls, 1.0 m apart is considered. The wall temperature is 400 K at $x = 0$ m and 1500 K at $x = 1.0$ m, respectively with an emissivity of 0.8. The gas medium is supposed to comprise non-gray 40% $H_2O$, 20% $CO_2$, and 40% transparent inert gas in which soot particulates are also suspended. The soot volume fraction is

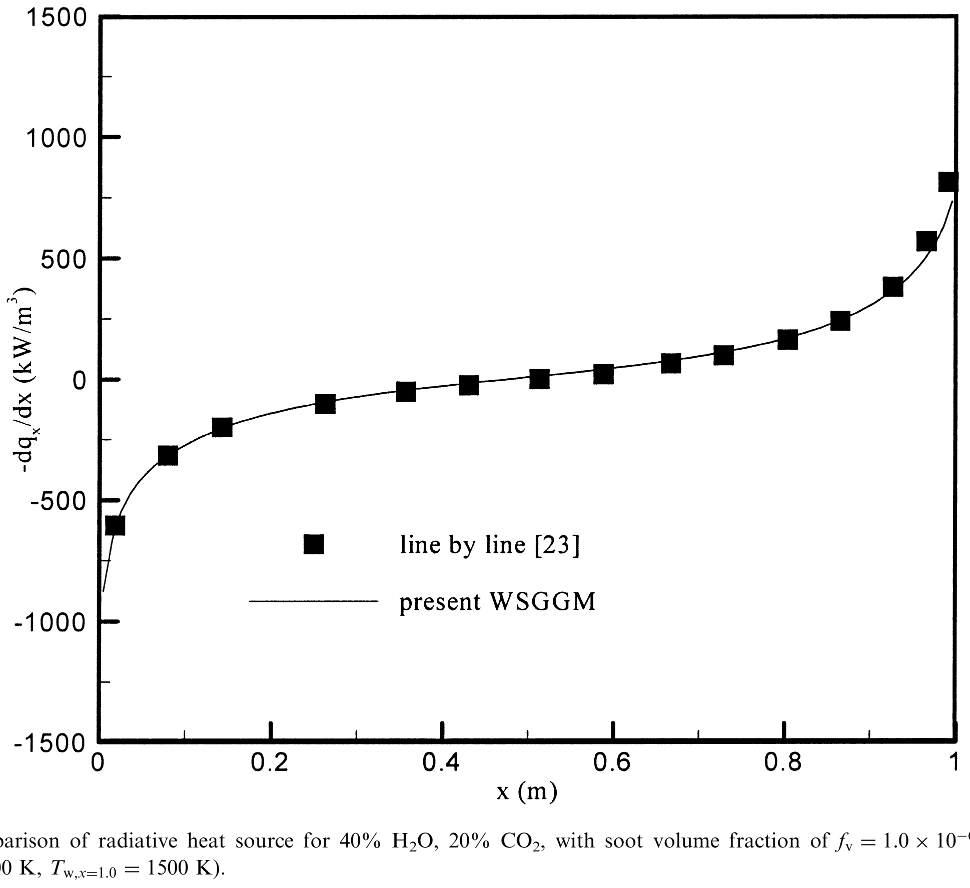


Fig. 2. Comparison of radiative heat source for 40% $H_2O$, 20% $CO_2$, with soot volume fraction of $f_v = 1.0\times10^{-6}$ at 1250 K. ($T_{w,x=0.0} = 400$ K, $T_{w,x=1.0} = 1500$ K).

set to be $f_v = 1.0 \times 10^{-6}$. The parameters required for the WSGG model for $CO_2$–$H_2O$ mixtures for the given partial pressure ratios are acquired from Smith et al. [8]. In Fig. 2 a variation of radiative heat source is plotted and compared with the solution obtained by using the line-by-line method [23]. Two results are seen to almost exactly match each other. Furthermore, a net heat flux at cold wall is found to be 112 kW/m$^2$ as in Denison [23]. This comparison suggests that the WSGGM derived here for the two phase mixture seems to be plausible.

Secondly, a pure scattering medium in a cylindrically symmetric geometry is conceived to examine the scattering phase function that is approximated by a finite series of Legendre polynomials as follows

$$\Phi(\hat{s}',\hat{s}) = \Phi(\cos\varphi) = \sum_{j=0}^{J} a_j P_j(\cos\varphi) \tag{29}$$

where the scattering angle $\varphi$ is the angle between incoming direction $\hat{s}'$ and outgoing direction $\hat{s}$. The expansion coefficients, $a_j$ are given by Kim and Lee [24]. The five types of scattering are considered in this study such that F2 and F3 are for forward scattering, while B1 and B2 are for backward scattering. As seen in Fig. 3, the results obtained here are in good agreement with those of Jendoubi et al. [25] and Kim and Baek [26] so that the validation of the numerical procedure is completed.

## 5. Results and discussion

In an industrial energy system the physical variables for the gas and particles are temporally as well as spatially varied going through various physical processes. For example, during a heating or devolatilization period the particle temperature is lower than the gas temperature, while in a burning period the particle temperature is higher than the gas temperature. Therefore, the two phase radiation under thermal non-equilibrium is ubiquitous from a view of practical applications. In the following, consequently, the two phase radiation in the thermal non-equilibrium is to be parametrically discussed in more detail.

As a first example, the geometry of two parallel walls previously discussed for validation is reconsidered. But in this case, in addition to 40% $H_2O$, 20%

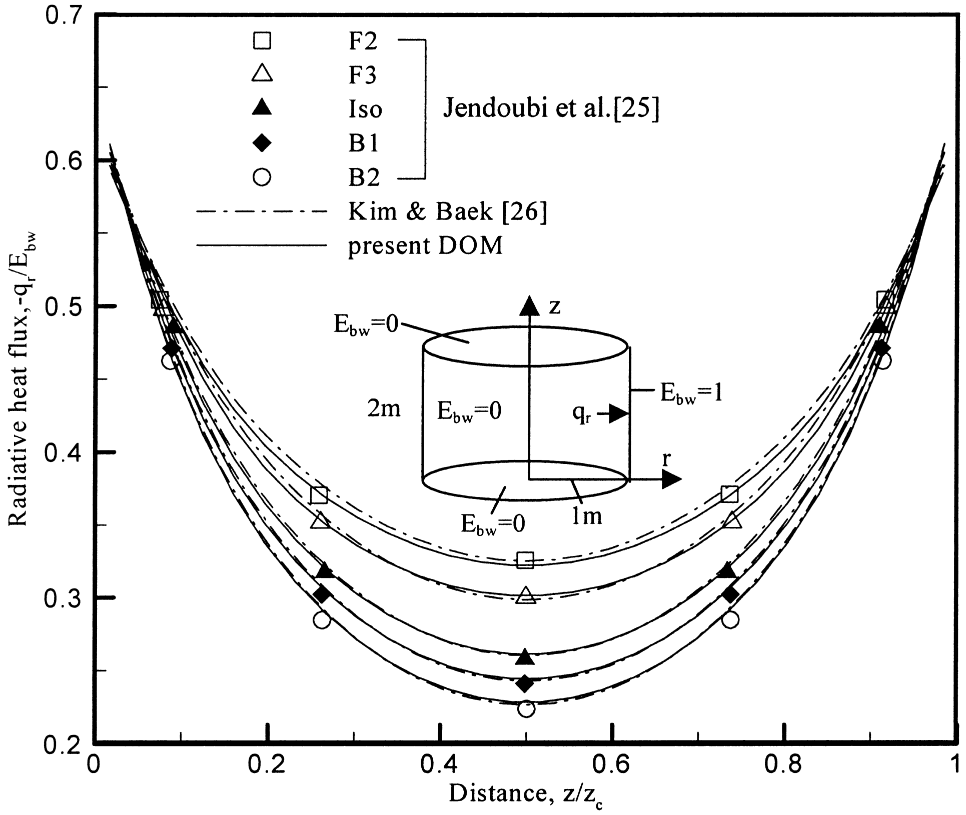


Fig. 3. Comparison of radiative heat flux in a right cylindrical enclosure.

$CO_2$, and 40% transparent inert gas with soot particulates, the scattering particles are supplementary suspended. The particle concentration is 0.1 kg/m$^3$ with emissivity of 0.8. The particle size is ranged in 50, 60, 70, 80, and 100 μm with 20% each by mass. The particle density is taken as 1300 kg/m$^3$ that is typical of coal particle. The unique difference of this work from the other previous ones resides in the fact that this study deals with the radiation in thermal non-equilibrium of which mixture consists of non-gray gases, gray soot particulates and particles.

In Fig. 4, when there are three types of temperature difference between gas and scattering particles given, the effects of scattering modes on the radiative heat flux are plotted. It must be noted that the soot temperature is set to be the same as the gas temperature $T_g = 1250$ K here, while the particle temperature is $T_p$. The forward, backward and isotropic scattering modes are compared with the non-scattering case. In general, as the particle temperature increases the radiative heat flux is observed to decrease in the region adjacent to the hot wall, while it increases in the vicinity of the cold wall regardless of scattering modes. This results from the fact that the positive radiative heat flux $q_x^+$ increases as the particle temperature increases, while the negative radiative heat flux $q_x^-$ does not increase as much as $q_x^+$, where the net radiative heat flux $q_x$ is the sum of the positive and negative heat fluxes, that is, $q_x = q_x^+ + q_x^-$. It is also found that the radiative heat flux is the highest for the case of non-scattering particles since the scattering itself does not contribute to the transformation of radiation into thermal >energy.

Next, an axisymmetric cylinder with 2 m diameter and 2 m length is considered. While its side wall temperature at $r = 1$ m is 1000 K with wall emissivity of 0.8, the bottom ($z = 0$ m) and top ($z = 2$ m) wall temperature is 400 K. The gas temperature is $T_g = 1000$ K, whereas the particle properties are the same as before. Only the isotropic scattering is considered here for brevity. In this case the soot particulates are omitted simply because their presence diminishes the radiation effects by the variation of gas and particles.

Since the radiative heat flux

$$q_r = \sum_k \int_{4\pi} I_k(s)\,d\Omega \tag{30}$$

and the divergence of the radiative heat flux for gas

$$\nabla\cdot q_r = \sum_k \nabla\cdot q_{r,k} = \sum_k \kappa_{g,k}\left[4\pi\left(w_k I_{b,g}\right) - \int_{4\pi} I_k(s)\,d\Omega\right] \tag{31}$$

are important quantities in the radiation, the effects of such physical conditions as non-gray gas composition and particle concentration on them are examined in an axisymmetric cylinder.

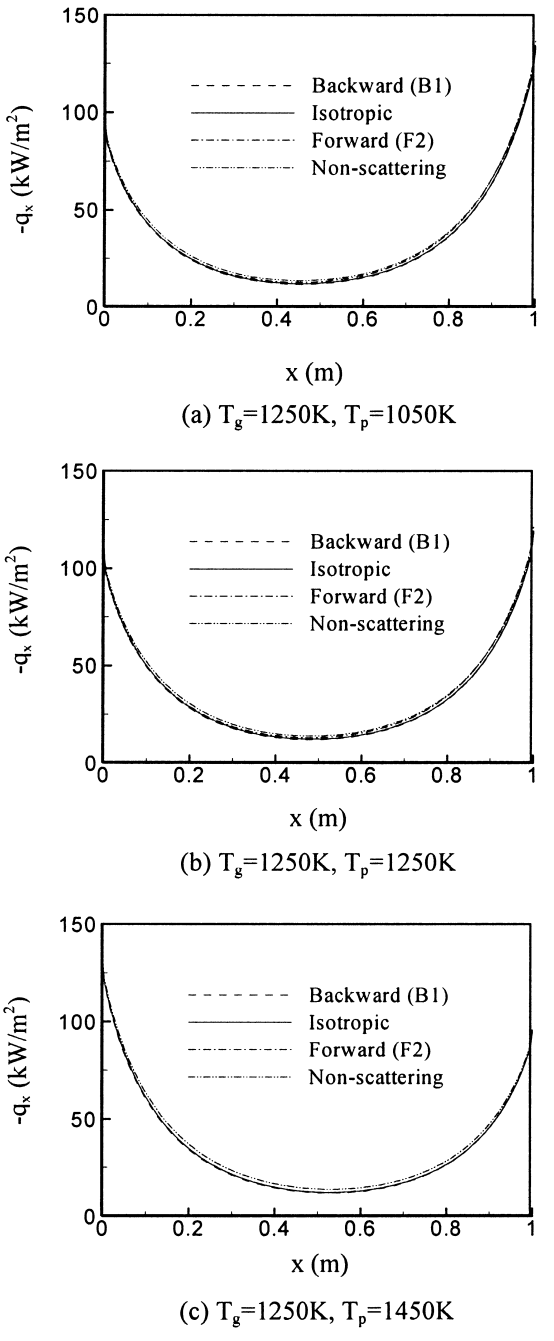


Fig. 4. The effects of scattering mode on the radiative heat flux for $T_g$ = 1250 K; (a) $T_p$ = 1050 K (b) $T_p$ = 1250 K (c) $T_p$ = 1450 K.

First of all, an applicability of the WSGG method to a mixture is examined when the particle temperature is the same as the gas temperature ($T_p = T_g = 1000$

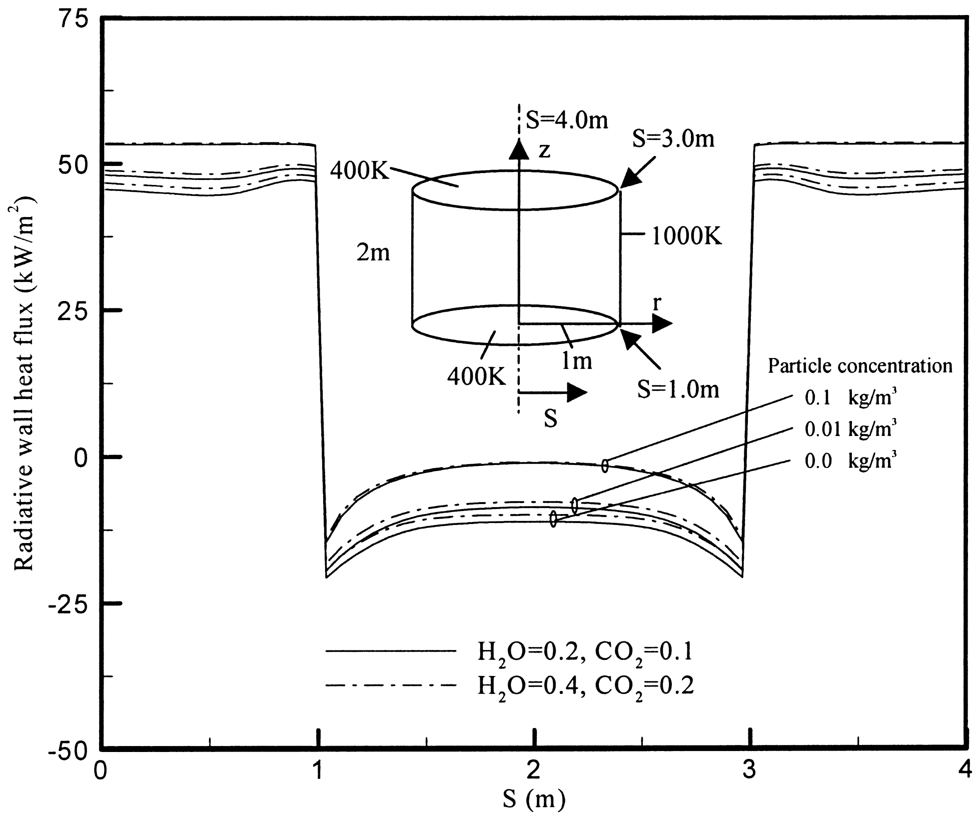


Fig. 5. The effects of gas composition and particle concentration on the radiative wall heat flux.

K). In Fig. 5, a variation of the radiative wall heat flux along distance $s$ is illustrated for three particle concentrations including the case without particles and two gas compositions. It is shown to increase as the particle concentration increases for a given gas composition, because the radiative intensity is more augmented due to the presence of particles. The effects of an increase in the non-gray gas compositions are also observed in the figure. When the gas composition becomes double, the radiative wall heat flux is also seen to increase. But the effect of gas composition is much reduced for the higher particle concentration of 0.1 kg/m$^3$, since the effect of the particle concentration is predominant. Compared with the case without particles, only 9% in the radiative wall heat flux increases for 0.1 kg/m$^3$ and 77% for 0.01 kg/m$^3$.

In Fig. 6, the effects of the particle temperature on the divergence of the radiative heat flux for gas are represented for $T_g = 1000$ K: (a) no particle, (b) $T_p = 800$ K, (c) $T_p = 900$ K, (d) $T_p = 1000$ K, (e) $T_p = 1100$ K, and (f) $T_p = 1200$ K. Particles with concentration of 0.1 kg/m$^3$ are suspended in 40% $H_2O$, and 20% $CO_2$, and 40% transparent gas. The divergence of the radiative heat flux for gas physically accounts for the net outflow of the radiation at a local control volume. As expected, the divergence of radiative heat flux for gas steadily decreases as the particle temperature increases, since more radiative energy is fed back to the gas.

The effects of particle concentration on the radiative heat flux at side wall and the divergence of radiative heat flux along radial direction at $z = 1$ m are examined for $T_p = 800$, 1000 and 1200 K in Fig. 7. For $T_p = 1000$ and 1200 K, as the particle concentration increases, the radiative heat flux at side wall increases while the divergence of radiative heat flux for gas along radial direction at $z = 1$ m decreases, since more radiation is supplied by hot particles. However, for $T_p = 800$ K which is lower than $T_g = 1000$ K, the radiative heat flux at side wall decreases and the divergence of radiative heat flux at $z = 1$ m increases, since the gas loses energy to the low-temperature particles.

Lastly, the effects of the non-gray gas composition on the radiative heat flux at side wall are explored for various particle concentrations for $T_p = 800$ K in Fig. 8 and for $T_p = 1200$ K in Fig. 9. When the non-gray composition becomes double, the radiative heat flux at side wall is seen to

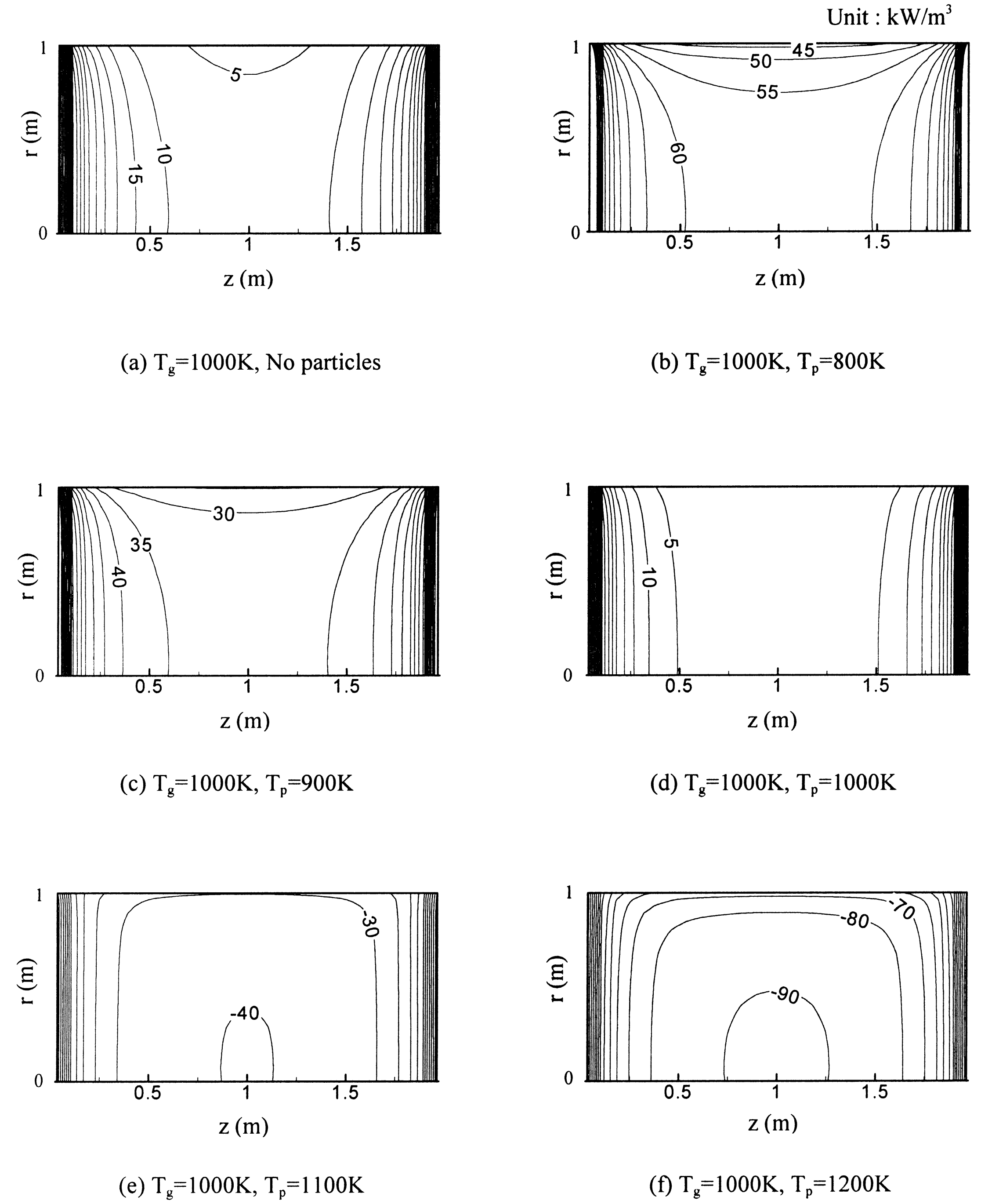


Fig. 6. Variation of the divergence of radiative heat flux for $T_g$ = 1000 K: (a) no particles, (b) $T_p$ = 800 K, (c) $T_p$ = 900 K, (d) $T_p$ = 1000 K, (e) $T_p$ = 1100 K, and (f) $T_p$ = 1200 K.

increase regardless of particle concentration as in Fig. 8 for which the particle temperature, $T_p = 800$ K is lower than the gas temperature, $T_g = 1000$ K. This results from the fact that the emission by high-temperature gas becomes predominant. But the radiative wall heat flux decreases as the particle concentration increases, since more energy is absorbed by low-temperature particles.

For the particle temperature, $T_p = 1200$ K which is higher than the gas temperature, $T_g = 1000$ K, the

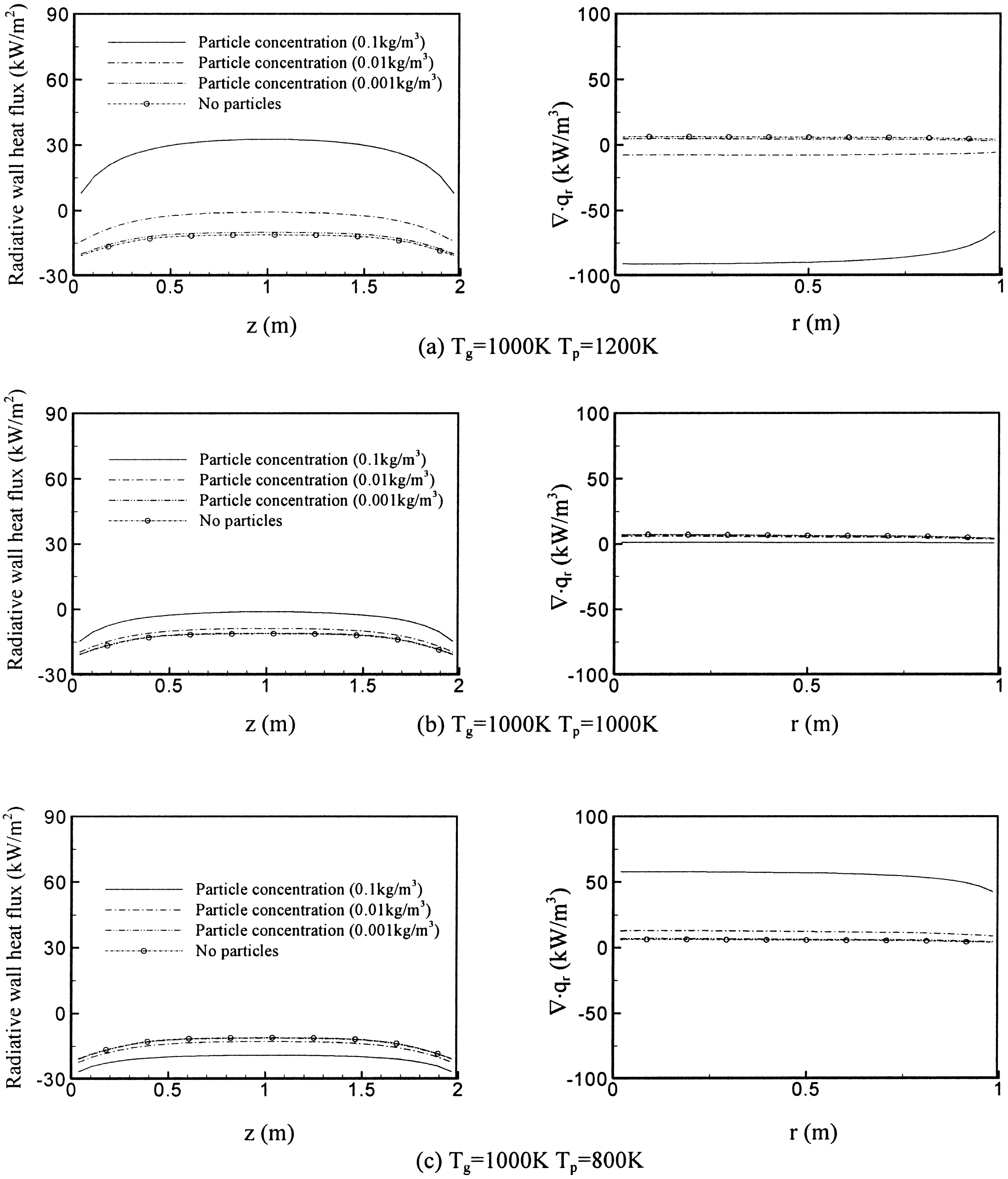


Fig. 7. The effects of particle concentration on the radiative wall heat flux and the divergence of radiative heat flux for $T_g = 1000$ K: (a) $T_p = 1200$ K, (b) $T_p = 1000$ K, and (c) $T_p = 800$ K.

radiative heat flux at side wall is observed to decrease even for high-temperature particle concentration of 0.1 kg/m$^3$ as shown in Fig. 9, when the non-gray composition becomes double. This is due to the heat blockage effects by more non-gray gas. But for lower particle concentration of 0.001 and 0.01 kg/m$^3$, the radiative

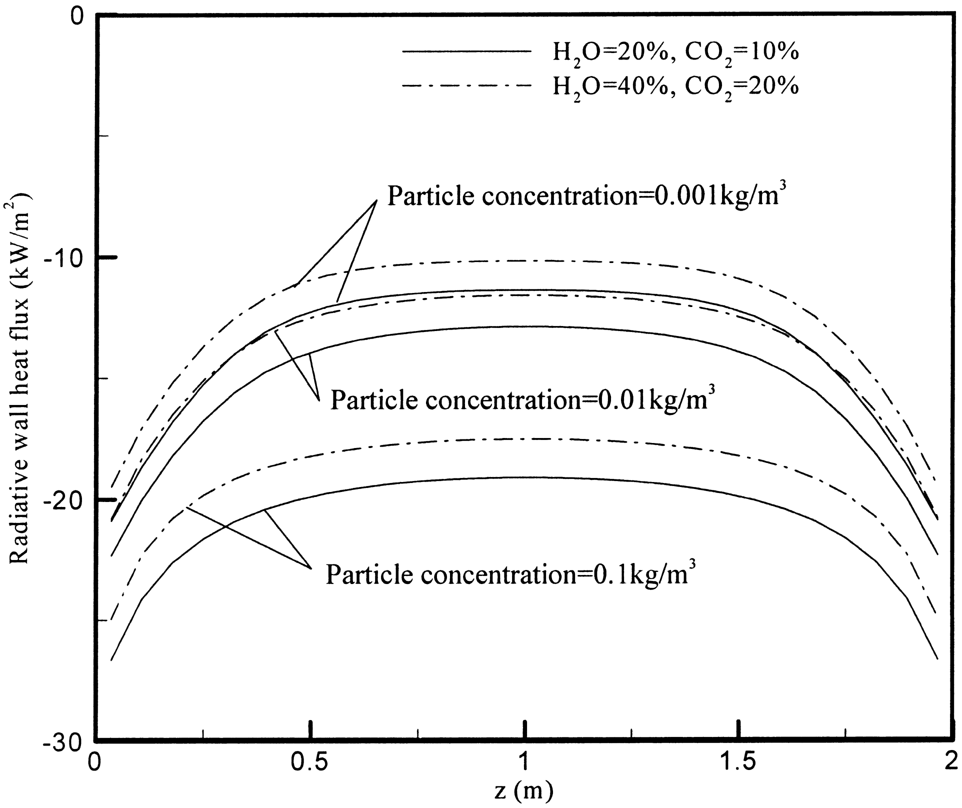


Fig. 8. The effects of gas composition on the radiative wall heat flux at side wall for $T_g = 1000$ K and $T_p = 800$ K.

heat flux at side wall is seen to increase, when the non-gray composition becomes double. This is because more radiation is emitted by more non-gray gas.

## 6. Conclusions

The weighted sum of gray gases model (WSGGM) has already been introduced by previous literature when there exists a non-gray gas only. In this study, it is extended to the two phase mixture while considering isotropic scattering as well as an-isotropic scattering. There has been no literature dealing with the radiation when gray soot particulates or particles are mixed with the non-gray gas. In order to calculate the radiation for this type of problem using WSGGM, the weighting factors for each gray band are required for both non-gray gas and particles. It was devised here that the weighting factors for non-gray gas and particles share the same functional such that

$$w_{p,k} = w_{g,k}(T_p)$$

even for the case that the gas and particles are not in thermal equilibrium.

The methodology derived here has been successfully validated for the problem with non-gray gas. Then, it was applied to a couple of problems of two phase radiation. Parametric study has been performed to gain an understanding of the effects of non-gray gas composition as well as particle concentration on the radiation. The effects of thermal non-equilibrium between gas and particles are also discussed in parallel with scattering effects by particles. The calculated result for soot-suspended medium agreed well with the benchmark solution. The parametric study showed that a variation in the gas concentration yielded a noticeable change in the radiative heat transfer when the suspended particle temperature is different from the gas temperature. New contribution of this study consists in an enhancement of applicability of the WSGGM non-gray model for two phase radiation.


## Acknowledgements

The authors wish to acknowledge the financial support of the Korea Research Foundation made in the program year of 1998 under the contract 1998-018-E00016.

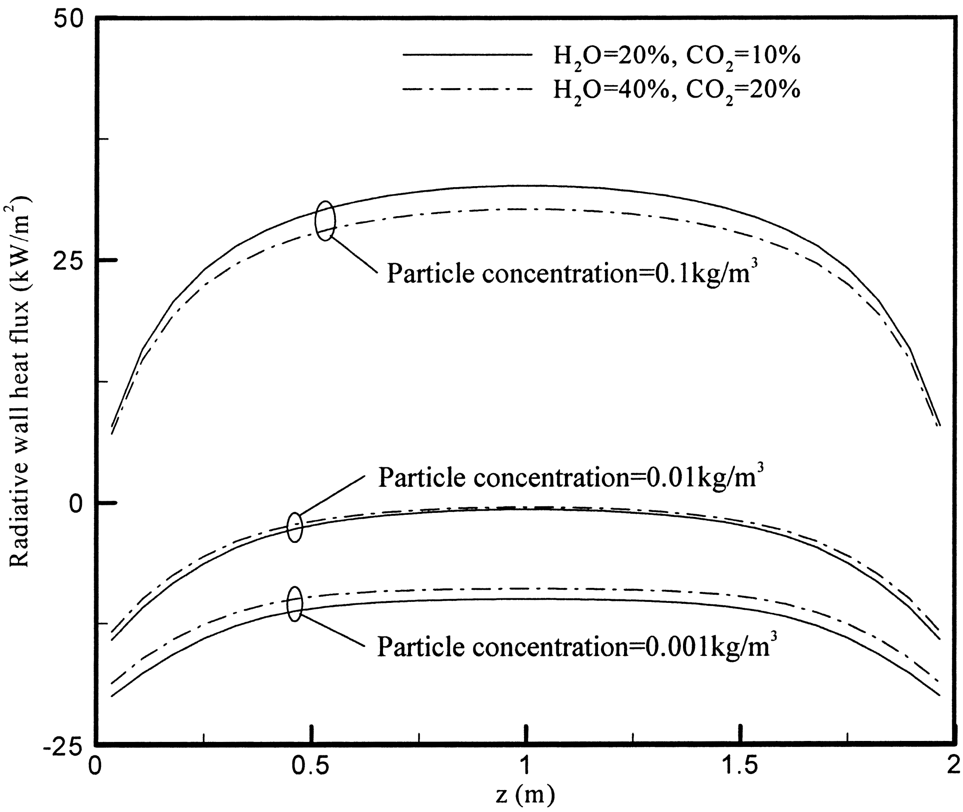


Fig. 9. The effects of gas composition on the radiative wall heat flux at side wall for $T_g = 1000$ K and $T_p = 1200$ K.

## References


[1] J.S. Truelove, The modelling of flow and combustion in swirled, pulverized-coal burners, in: Twentieth Symposium (International) on Combustion, 1984, pp. 523–530.

[2] F.C. Lockwood, T. Mahmud, The prediction of swirl burner pulverized coal flames, in: Twenty Second Symposium (International) on Combustion, 1988, pp. 165–173.

[3] E.H. Chui, P.M.J. Hughes, G.D. Raithby, Implementation of finite volume method for calculating radiative transfer in a pulverized fuel flame, Combustion Science and Technology 92 (1993) 225–242.

[4] J.H. Park, S.W. Baek, S.J. Kwon, Analysis of a gas–particle direct-contact heat exchanger with two-phase radiation effect, Numerical Heat Transfer, Part A 33 (1998) 701–721.

[5] H.C. Hottel, A.F. Sarofim, Radiative Transfer, McGraw-Hill, New York, 1967.

[6] C.E. Choi, S.W. Baek, Numerical analysis of a spray combustion with non-gray radiation using weighted sum gray gases model, Combustion Science and Technology 115 (1996) 297–315.

[7] F. Liu, H.A. Becker, Y. Bindar, A comprehensive study of radiative heat transfer modelling in gas-fired furnaces using the simple gray gas and the weighted-sum-of-gray-gases models, International Journal of Heat and Mass Transfer 41 (1998) 3357–3371.

[8] T.F. Smith, Z.F. Shen, J.N. Friedman, Evaluation of coefficients for the weighted sum of gray gases model, ASME Journal of Heat Transfer 104 (1982) 602–608.

[9] A. Coppalle, P. Venisch, The total emissivities of high-temperature flames, Combustion and Flame 49 (1983) 101–108.

[10] N. Lallemant, A. Sayre, R. Weber, Evaluation of emissivity correlations for $H_2O$–$CO_2$–$N_2$/air mixtures and coupling with solution methods of the radiative transfer equation, Progress in Energy and Combustion Science 22 (1996) 543–574.

[11] M.K. Denison, B.W. Webb, *k*-Distribution and weighted-sum-of-gray-gases — a hybrid model, Proceedings of the Tenth International Heat Transfer Conference 2 (1994) 19–24.

[12] J. Hruby, R. Steeper, G. Evans, C. Crowe, An experimental and numerical study of flow and convective heat transfer in a freely falling curtain of particles, Journal of Fluid Engineering 110 (1988) 172–181.

[13] K. Ohtake, K. Okazaki, Optical CT measurement and mathematical prediction of multi-temperature in pulverized coal combustion fluid, International Journal of Heat and Mass Transfer 31 (1988) 397–405.

[14] H. Farzan, R.H. Essenhigh, High intensity combustion of coal, in: Nineteenth Symposium (International) on Combustion, 1982, pp. 1105–1111.

[15] D.W. Mackowski, R.A. Altenkirch, R.E. Peck, T.W. Tong, A method for particle and gas temperature measurement in laboratory-scale pulverized-coal flames, Combustion Science and Technology 31 (1983) 139–153.
[16] B.W. Butler, M.K. Denison, B.W. Webb, Radiation heat transfer in a laboratory-scale, pulverized coal-fired reactor, Experimental Thermal and Fluid Science 9 (1994) 69–79.
[17] M.F. Modest, Radiative Heat Transfer, McGraw-Hill, New York, 1993.
[18] M.K. Denison, B.W. Webb, Modelling of radiative transfer in pulverized coal-fired furnaces: effect of differing particle and gas temperature, Proceedings of Sixth International Symposium on Transport Phenomena in Thermal Engineering 1 (1993) 191–196.
[19] M.M. Yuen, A. Ma, Evaluation of total emittance of an isothermal nongray absorbing, scattering gas–particle mixture based on the concept of absorption mean beam length, ASME Journal of Heat Transfer 114 (1992) 653–658.
[20] T.H. Song, Comparison of engineering models of nongray behavior of combustion products, International Journal of Heat and Mass Transfer 36 (16) (1993) 3975–3982.
[21] R.D. Skocypec, D.V. Walters, R.D. Buckius, Spectral emission measurements from planar mixtures of gas and particulates, ASME Journal of Heat Transfer 109 (1987) 151–158.
[22] B.G. Carlson, K.D. Lathrop, in: H. Greenspan, et al. (Eds.), Computing Methods in Reactor Physics, Gordon and Breach, New York, 1968.
[23] M.K. Denison, A spectral line-based weighted-sum-of-gray-gases model for arbitrary RTE solvers. Ph.D Thesis. Department of Mechanical Engineering, Brigham Young University, 1994.
[24] T.K. Kim, H. Lee, Radiative heat transfer in two-dimensional anisotropic scattering media with collimated incidence, Journal of Quantitative Spectroscopy and Radiative Transfer 42 (3) (1989) 225–238.
[25] S. Jendoubi, H.O. Lee, T.K. Kim, Discrete ordinate solutions for radiative participating media in a cylindrical enclosure, Journal of Thermophysics and Heat Transfer 7 (2) (1993) 213–219.
[26] M.Y. Kim, S.W. Baek, Analysis of radiative transfer in cylindrical enclosures using the finite volume method, Journal of Thermophysics and Heat Transfer 11 (2) (1997) 246–252.